Δk-Radar Equivalent of Interferometric SAR's: A Theoretical Study for Determination of Vegetation Height

Kamal Sarabandi, *Senior Member, IEEE*

***Abstract*— In this paper the theoretical aspects of estimating vegetation parameters from SAR interferometry are presented. In conventional applications of interferometric SAR (INSAR), the phase of the interferogram is used to retrieve the location of the scattering phase center of the target. Although the location of scattering phase center for point targets can be determined very accurately, for a distributed target such as a forest canopy this is not the case. For distributed targets the phase of the interferogram is a random variable which in general is a function of the system and target attributes. To relate the statistics of the interferogram phase to the target attributes, first an equivalence relationship between the two-antenna interferometer system and an equivalent Δk radar system is established. This equivalence relationship provides a general tool to related the frequency correlation function (FCF) of distributed targets, which can conveniently be obtained experimentally, analytically, or numerically, to the phase statistics of the interferogram. An analytical form for the p.d.f. of the interferogram phase is obtained in terms of two independent parameters: 1) ζ: mean phase and 2) α: degree of correlation. ζ is proportional to the scattering phase center and α is inversely proportional to the uncertainty with which ζ can be estimated. It is shown that α is directly related to the FCF of the distributed target which in turn is a function of scattering mechanisms and system parameters. It is also shown that for a uniform closed canopy the extinction and the physical height of the canopy top can be estimated very accurately. Some analytical and numerical simulations are demonstrated.**

I. Introduction

VEGETATION cover on the earth's surface is an important factor in the study of global changes. The total vegetation biomass is the most influential input to models for terrestrial ecosystems and atmospheric chemistry. Monitoring parameters such as the total vegetation biomass, total leaf area index, and rate of deforestation is vital to keep our planet capable of supporting life. Microwave remote sensing techniques offer a unique opportunity to probe vegetation canopies at different depths. Since a forest stand is a very complicated random medium with many attributes that influence the forest radar response, accurate estimation of the forest physical parameters requires a large number of independent radar observations (multifrequency and multipolarization backscatter) in conjunction with some a priori information about the forest stand [1]–[4]. The use of polarimetric synthetic aperture radars as active sensors to survey forested areas has reached a level of maturity. Despite considerable advancement in retrieving the canopy parameters from multipolarization and multifrequency backscatter data, an unsupervised reliable inversion algorithm has not yet been developed. With the recent advances in the development of interferometric SAR's [5]–[10], another set of independent radar observation has become available for the estimation of vegetation biophysical parameters.

The interferometric technique relies on a coherent imaging process to find the range or distance to the scattering phase center of the scatterers in the radar image. Based on this principle, there are two standard approaches for extracting topographical information using synthetic aperture radars. In one approach, SAR systems equipped with two separate antennas mounted on the SAR platform are used to generate two complex co-registered images from two slightly different aspect angles. The phase difference calculated from the cross product of the two complex images, referred to as an interferogram [6], is processed to estimate the height information. In the second approach the interferogram is formed using two successive images taken by a single SAR with almost the same viewing geometry [7], [8]. It is shown that the phase of the interferogram is proportional to the wavelength, slant range, look angle, distance between the antennas (baseline distance), orientation of the antennas with respect to each other, and the height of the scattering phase center above a reference line [5], [9]. For nonvegetated terrain, the scattering phase centers are located at or slightly below the surface depending upon the wavelength of the SAR and the dielectric properties of the surface media. Whereas for vegetated terrain, these phase centers lie at or above the surface depending upon the wavelength of the SAR and the vegetation attributes. Although it is expected that for vegetated surfaces the temporal decorrelation would hamper repeat-pass interferometry from producing the location of scattering phase center, experimental investigations has shown that even after 18 days the correlation associated with forested area can be as high as 0.5 [11], [12].

The significant vegetation attributes are 1) the type of vegetation; 2) the quantity or biomass of the vegetation; and 3) the dielectric properties of the vegetation. As pertains to SAR interferometry, the type of vegetation refers to the structural attributes of vegetation elements and includes the shapes and sizes of foliage and woody stems relative to wavelength and their three-dimensional organizational structure. The biomass refers to attributes such as the height of the vegetation,

Manuscript received April 15, 1996; revised October 7, 1996.

The author is with the Radiation Laboratory, Department of Electrical Engineering and Computer Science, The University of Michigan, Ann Arbor, MI 48109-2122 USA (e-mail: saraband@eecs.umich.edu).

Publisher Item Identifier S 0196-2892(97)05499-5.

the thickness and density of the crown layer that contains foliage and stems, and the number of plants per unit area. The dielectric properties of the vegetation elements determine scattering and propagation through the media; these may vary with time due to seasonal changes in plant physiology and the phase of water (liquid or frozen) or due to the presence of water films resulting from intercepted precipitation or dew.

The main objective of this paper is to establish a thorough understanding of the relationship between the INSAR parameters and the vegetation attributes and the accuracy with which the vegetation scattering phase center can be measured. To accomplish these goals an equivalence between INSAR and Δk-radar techniques is established which facilitates numerical simulations and controlled experiments using scatterometers. Monte Carlo simulation of a forest canopy which preserves the absolute phase of the radar backscatter allows for quantifying the role of vegetation attributes in determining the location of the scattering phase centers as measured by SAR interferometry.

II. Δk-Radar Equivalent of an INSAR

In this section an equivalence relationship between an interferometric SAR and a Δk-radar is obtained. As will be shown later the statistics of the phase of the interferogram or equivalently the location of the scattering phase center and its statistics is a very strong function of the location and number density of the forest constituent particles and their dielectric and scattering properties. Understanding the relationship between the tree height and the corresponding location of the scattering phase centers requires numerical simulations (Monte Carlo simulation of a fractal generated forest stand) or controlled experiments using scatterometers. The scattering phase center of a target can also be obtained using a Δk-radar assuming that the incidence angle is known. Evaluation of the scattering phase centers using frequency shift can easily be accomplished in a numerical simulation or in a controlled experiment using a wideband scatterometer.

To demonstrate the equivalence between an INSAR and a Δk-radar consider a two-antenna interferometer as shown in Fig. 1. In this scheme one of the antennas is used as the transmitter and receiver and the other one is used only as the receiver, the phase of the interferogram (ϕ) is related to the difference in path lengths from the antennas to the scattering phase center (δ) by

$$\delta = \frac{\lambda_0}{2\pi}\phi \tag{1}$$

where $\lambda_0 = c/f_0$ is the wavelength (in repeat-pass interferometry the 2π factor in (1) must be replaced by 4π). Having calculated δ from (1) and knowing the baseline distance B and baseline angle α, the look angle θ can be computed from

$$\sin(\theta - \alpha) \approx \frac{-\delta}{B}. \tag{2}$$

Referring to Fig. 1 it can easily be shown that the height of the scattering phase center, with respect to an arbitrary reference level, is given by

$$h = H - r[\cos(\alpha)\cos(\theta - \alpha) - \sin(\alpha)\sin(\theta - \alpha)]. \tag{3}$$

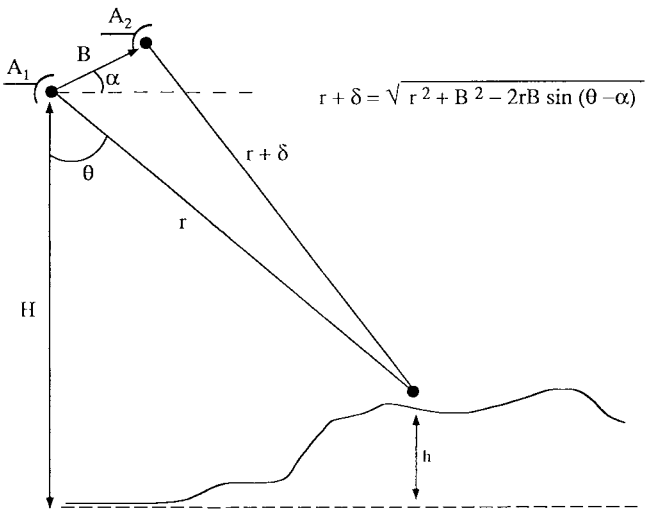

Fig. 1. Geometry of a two-antenna interferometer.

The accuracy in height estimation using this method is directly proportional to the accuracy in the measurement of the interferogram phase. The uncertainty in phase measurements is caused by two factors: (1) systematic errors, and (2) indeterministic errors. The sources of systematic errors are image misregisteration and lack of maintaining the geometry of the interferometer. The source of indeterministic error is fading. Basically the backscatter signal from a distributed target including many scatterers decorrelates as the incidence angle changes.

Now let us consider a radar capable of measuring the backscatter at two slightly different frequencies $f_1 = f_0$ and $f_2 = f_0 + \Delta f$. Denoting the phase difference between the two backscatter measurements by ϕ, it can be shown that

$$\phi = 2\Delta k r = 4\pi \Delta f r/c \tag{4}$$

where c is the speed of light and r is the radar distance to the target scattering phase center. Comparing (4) with (1) and (2) the desired relationship between the Δk-radar and INSAR can be obtained. Basically by requiring the backscatter phase differences, once obtained from a small change in the aspect angle and the other one obtained from a small change in the frequency of operation, be identical for both approaches we have

$$\Delta f = f_0 \frac{B}{2r}\sin(\theta - \alpha). \tag{5}$$

Noting that $r = H/\cos(\theta)$, it can easily be shown that Δf is rather insensitive to variations in incidence angle over the angular range 30°–60°. For example, a C-band (5.3 GHz) interferometer with a horizontal baseline distance 2.4 m at an altitude 6 Km is equivalent to a C-band Δk-radar with Δf = 530 KHz.

The equivalence relation given by (5) is derived based on a single target. In regard to this relationship there are two subtle issues that require clarification. In almost all practical situations the scatterers are located above a ground plane which give rise to three significant scattering terms besides the direct backscatter. These include the bistatic scattering

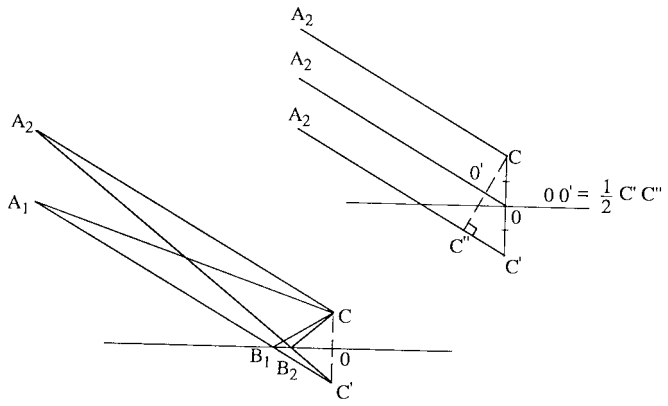

Fig. 2. Ray path configuration of the single-bounce ground-target scattering mechanism for a two-antenna interferometer.

from the target reflected from the ground plane, the bistatic scattering from the target when illuminated by the reflected wave, and the backscatter reflected by the ground plane when the target is illuminated by the reflected wave. The last term can be regarded as the direct backscatter of the incident wave from the image target and therefore the equivalent Δk-radar can accurately predict the interferometric phase associated with this term. However, for the other two scattering terms (single-bounce terms), the validity of the equivalence relationship is not obvious. Suppose a two-antenna interferometer, as shown in Fig. 2, is illuminating a target at point C above the ground plane. For the equivalent Δk-radar located at A_1, the interferometric phases of the two single-bounce terms (ϕ_b) are identical and are given by

$$\phi_b = \Delta k(A_1B_1 + B_1C + CA_1) = 2\Delta k A_1 O. \tag{6}$$

Equation (6) indicates that the location of the scattering phase center for the ground-bounce terms appears at the ground interface for the Δk-radar. The interferometric phase of the two single-bounce terms for the two-antenna system can be obtained from

$$\phi_b' = \angle 2e^{ik(A_1C+CB_1+B_1A_1)} - \angle(e^{ik(A_1C+CB_2+B_2A_2)} + e^{ik(A_1B_1+B_1C+CA_2)}).$$

Noting that $B_1C = B_1C', B_2C = B_2C'$, and after some simple algebraic manipulation, it can be shown that

$$\phi_b' = \frac{k}{2}[(A_1C + A_1C') - (A_2C + A_2C')].$$

Referring to Fig. 2, it can easily be shown that $C'C'' = 2OO'$ and therefore $A_2C + A_2C' = 2A2O$. Similarly, it can be shown that $(A_1C + A_1C') = 2A_1O$, thus

$$\phi_b' = k(A_1O - A_2O).$$

which indicates that the location of scattering phase center for the two single-bounce terms is at O. Therefore the equivalence relation (5) guarantees that $\phi_b = \phi_b'$.

The second issue pertains to the validity of the equivalence relation with regard to multiple scattering terms. As mentioned earlier the equivalence relationship is derived based on a single target and therefore it would be valid for a random medium, if the overall backscatter is dominated by the first-order scattering mechanisms. To demonstrate that the equivalent Δk-radar provides the location of the scattering phase center accurately even in the presence of multiple scattering, consider two scatterers located at two arbitrary points C and D within a resolution cell. For an INSAR whose antennas are at points A_1 and A_2, the interferometric phase associated with the second order scattering terms is calculated from

$$\phi_{\text{INSAR}}^{(2)} = \angle 2e^{ik(A_1C+CD+DA_1)} - \angle(e^{ik(A_1C+CD+DA_2)} + e^{ik(A_1D+CD+CA_2)}).$$

In derivation of the above equation, the reciprocity theorem is used which indicates that the second-order scattering amplitude obtained from the interaction between particle C and particle D is equal to that obtained from the interaction between particle C and particle D. As before it can easily be shown that

$$\phi_{\text{INSAR}}^{(2)} = \frac{k}{2}[(A_1C + A_1D) - (A_2C + A_2D)].$$

Let us define M as point in the middle of CD line. Since the distance between the antennas and the scatterers are much larger than the distance between the scatterers, we have

$$\phi_{\text{INSAR}}^{(2)} = k(A_1M - A_2M)$$

which indicates that the phase center of the second order term apperas at the midpoint between the two scatterers. For a Δk-radar at A_1 the same second order phase term is given by:

$$\phi_{\Delta k}^{(2)} = \Delta k(A_1C + CD + DA_1).$$

Noting that $A_1C + A_1D \approx A_1M$ and $CD \ll A_1M$, the above expression reduces to

$$\phi_{\Delta k}^{(2)} = 2\Delta k A_1 M. \tag{7}$$

Equation (7) shows that the location of scattering phase center measured by a Δ-k radar is at M as well.

What remains to be shown is the algorithm by which the target height can be extracted from an equivalent Δk-radar. Let us consider a random collection of scatterers within a range and azimuth resolution cell illuminated by a plane wave as shown in Fig. 3. The height of the scattering phase center for this collection can be considered to be the algebraic sum of the physical height of the pixel center and a residual apparent height of the scatterers which is a complex function of particles and radar attributes. Suppose there are M scatterers within a resolution cell. Let s_n denote the scattering amplitude of the nth scattering component of the ensemble which can represent the direct backscattering from a particle, a multiple scattering term between a number of the scatterers in the ensemble, or a bistatic scattering term reflected from the ground plane. Without loss of generality let us assume that the phase reference is on the reference plane just below the pixel center (see Fig. 3). The total backscattered field is the

coherent sum of all the scattering components which can be obtained from

$$E^s = \frac{e^{ik_0 r}}{r} \sum_{n=1}^{N} s_n e^{-i2k_0 r_n}. \tag{8}$$

where r is the distance from the origin to the observation point, r_n is the total round trip path length difference between a ray traveled to the origin and the ray corresponding to the nth scattering component. Note that a time convention of $e^{-i\omega t}$ has been assumed and suppressed. The equivalent problem is to replace the collection of the random particles and the underlying ground plane with an equivalent scatterer placed at the scattering phase center whose backscattering amplitude is denoted by $S_e = |S_e| \exp(i\Phi_e)$. In this case the backscattered field is given by

$$E^s = \frac{e^{ik_0 r}}{r} S_e e^{-2ik_0 h \cos(\theta)}.$$

Computing the phase of the backscattered field (Φ^s) from (8) and noting that the phase calculation is modulo 2π, the height of the scattering phase center can be obtained from

$$-2k_0 h \cos(\theta) + \Phi_e = 2m\pi + \Phi^s. \tag{9}$$

However, in computation of h from (9) two important parameters, namely m and Φ_e are missing. This problem could be rectified, if a radar measurement from the same collection of particles and the same viewing angle but at a slightly different frequency were available. Suppose the change in frequency is small enough so that the change in the phase of the scattering amplitudes is negligible. In this case the change in the phase of the scattered field $(\phi = \Phi_2^s - \Phi_1^s)$ due to the change in the wavenumber $(\Delta k = k_2 - k_1)$ is basically dominated by the path length differences and it can easily be shown that

$$h = \frac{-1}{2\cos(\theta)} \frac{\phi}{\Delta k}. \tag{10}$$

Equation (10) is the fundamental basis for extraction of height information from a two-frequency radar. It should be emphasized that in this process the incidence angle must be known which is the case in a numerical simulation or in a measurement using a narrow beam scatterometer system. Since the shift in frequency is very small (less than 0.1% of center frequency), the scattering amplitude terms s_n do not change when the frequency is changed from f_1 to f_2 and therefore they need not be computed twice in a numerical simulation. However, the phase terms associated with the path length differences must be modified by replacing k_0 with $k_0 + \Delta k$.

Expressing the measured phase in degrees, the difference in slant range $(\Delta r = h\cos(\theta))$ in meters, and the difference in frequency (Δf) in MHz, (8) can be rewritten as

$$\phi = 2.4 \Delta r \Delta f. \tag{11}$$

Therefore if the uncertainty in the phase calculation/measurement is 1° and a distance resolution of 1 m is required, a minimum frequency shift of 416.66 KHz is needed assuming that the uncertainty in phase calculation/measurement is independent of frequency shift

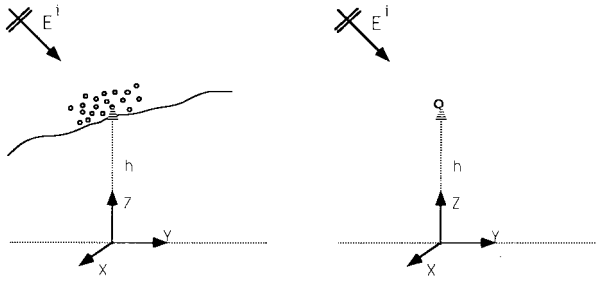

Fig. 3. A random collection of M scatterers above a ground plane and its equivalent scatterer.

(a wrong assumption). Using this frequency shift the unambiguous range of 360 m can be achieved noting that the phase is measured modulo 360°. The uncertainties in height estimation using a Δk-radar can easily be obtained as the relationship between h and θ is explicitly expressed by (10). It can easily be shown that the uncertainty in height due to the lack of accuracy in the knowledge of the incidence angle is given by:

$$\delta h = h \tan(\theta) \delta\theta.$$

For uncertainties in incidence angle as high as 3°, the error in height is 5% of h at $\theta = 45°$.

Through the combination of two or more frequency shifts, an unambiguous height profile with fine resolution can be achieved. The resolution in height estimation using Δk-radar is characterized by the frequency correlation function of the target as will be discussed next. Equation (10) indicates that accuracy in the height measurement increases as the frequency shift increases. On the other hand as the frequency shift (baseline distance) increases the phase shift caused by the path length differences will change in a nonlinear and random fashion which causes an uncertainty in the measurement of distance (height). Hence there may exist a critical frequency shift for which the finest height resolution for a given distributed target can be achieved. This critical frequency shift is the counterpart of a critical baseline distance in an interferometer for which the finest height resolution for the same distributed target is achievable.

III. Statistical Analysis

In estimating the height of the scattering phase center of a distributed target using (11), random fluctuations of the calculated/measured phase as a function of frequency due to fading must be considered. In this section the effect of random position of the scatterers on the height estimation is studied. Also a procedure for calculation of the critical frequency shift (baseline distance) in terms the statistical properties of the distributed target is outlined. Phase statistics of polarimetric backscatter response of kdistributed targets for single- and multi-look can be found in literature [14]–[16]. The statistical analysis of interferometric phase given here parallels the method given in [14]. For a random collection of particles the scattered field given by (8) is a complex random variable. Since the location of the scatterers in the illuminated volume is random, the process describing the scattered field is a Wiener

process [13]. If the number of scattering components M is large, the central limit theorem mandates that the process is Gaussian. Let us denote the scattered field at f_1 and f_2 by $E_1^s = X_1 + iX_2$ and $E_2^s = X_3 + iX_4$, respectively, where X_j denotes the real or imaginary part of the scattered fields. These quantities are jointly Gaussian and can be represented by a four-component random vector $\boldsymbol{X}$. The joint probability density function (pdf) of the random vector can be fully characterized from a 4×4 symmetric positive definite matrix known as the covariance matrix Λ whose entries are given by

$$\lambda_{ij} = \lambda_{ji} = \langle X_i X_j \rangle \qquad i,j \in \{1, \cdots, 4\}.$$

It has been shown that the entries of the covariance matrix for the Wiener process satisfy the following conditions [14]:

$$\lambda_{11} = \lambda_{22} = \langle X_1^2 \rangle = \langle X_2^2 \rangle, \tag{12}$$
$$\lambda_{12} = \langle X_1 X_2 \rangle = 0, \tag{13}$$
$$\lambda_{33} = \lambda_{44} = \langle X_3^2 \rangle = \langle X_4^2 \rangle, \tag{14}$$
$$\lambda_{34} = \langle X_3 X_4 \rangle = 0, \tag{15}$$
$$\lambda_{13} = \lambda_{24} = \langle X_1 X_3 \rangle = \langle X_2 X_4 \rangle, \tag{16}$$
$$\lambda_{14} = -\lambda_{23} = \langle X_1 X_4 \rangle = -\langle X_2 X_3 \rangle. \tag{17}$$

In the same paper [14] it is also shown that the pdf for the difference between phases of E_2^s and E_1^s (for a single-look case) is related to the elements of the covariance matrix and is given by

$$f_\Phi(\phi) = \frac{1-\alpha^2}{2\pi[1-\alpha^2\cos^2(\phi-\zeta)]} \cdot \left\{ 1 + \frac{\alpha\cos(\phi-\zeta)}{\sqrt{1-\alpha^2\cos^2(\phi-\zeta)}} \cdot \left[\frac{\pi}{2} + \tan^{-1}\frac{\alpha\cos(\phi-\zeta)}{\sqrt{1-\alpha^2\cos^2(\phi-\zeta)}} \right] \right\} \tag{18}$$

where

$$\alpha = \sqrt{\frac{\lambda_{13}^2 + \lambda_{14}^2}{\lambda_{11}\lambda_{33}}}, \quad \zeta = \tan^{-1}\frac{\lambda_{14}}{\lambda_{13}}.$$

The parameter α is known as the degree of correlation and can vary from 0 to 1. When the scattered fields are completely correlated $\alpha = 1$ and the pdf of ϕ is a delta function. In this case the calculation of the height from (10) has no error in principle when the effect of thermal noise is ignored. The parameter ζ is known as the coherent phase difference and can vary from $-\pi$ to π. For $\phi = \zeta$ the pdf assumes its maximum and this point corresponds to the average height of the scattering phase center for a uniform distributed target over a flat ground plane.

In this analysis the objective is to establish a relationship between a desired height resolution and the corresponding required frequency shift for a given error probability criterion. The Wiener processes considered in this problem satisfy one more condition beyond those given by (12)–(17). This condition can be derived by noting that the required frequency shift for the height estimation is much smaller than the operating center frequency of the radar, therefore it is expected that backscattered power carried by the two processes be equal. This requirement renders the following condition:

$$\lambda_{11} = \lambda_{33}. \tag{19}$$

Let us define the normalized correlation function of the process by

$$R(\Delta f) = \frac{|\langle E_1 E_2^* \rangle|}{\langle |E_1|^2 \rangle} \tag{20}$$

which is also known as the frequency correlation function [17]. Using (16), (17), and (19), it can easily be shown that

$$R(\Delta f) = \alpha. \tag{21}$$

It is interesting to note that the maximum of the normalized frequency correlation function occurs at $\Delta f = 0 (dR/d\Delta F|_{\Delta f=0} = 0)$, hence $\alpha = 1$ to the first order in Δf. In other words for small variation of frequency the pdf of the phase difference is very narrow which ensures accurate estimation of the height. As expected, when Δf increases, $\alpha = R(\Delta f)$ approaches zero which corresponds to a uniform distribution for the phase difference. In this case the probability of error in the height estimation is close to unity.

To quantify the accuracy of the height estimation for a given distributed target, let us assume that the normalized frequency correlation function of the target is known. In this case only the coherent phase difference (ζ) is missing to fully characterize the pdf of the phase difference. The objective is to estimate ζ from which the mean height can be obtained from

$$\overline{h} = \frac{-\zeta}{2.4\Delta f\cos(\theta)}. \tag{22}$$

However, the difficulty in calculation of $\overline{h}$ is that only one measurement of the phase for each pixel is available. Suppose $\delta\phi = \phi - \zeta$ represents the deviation in the phase measurement which corresponds to an error in height measurement given by

$$\delta h = \frac{\delta\phi}{2.4\Delta f\cos\theta} \tag{23}$$

where δh is in meters, $\delta\phi$ is in degrees, and Δf is in megahertz. The uncertainty in the estimation of height can be quantified according to a prescribed error probability criterion. For example, $\delta\phi$ can be chosen such that the probability of measuring the phase within the $\delta\phi$ neighborhood of the coherent phase difference to be 90%, that is

$$P(\phi \in [\zeta - \delta\phi, \zeta + \delta\phi]) = 0.9.$$

Hence, using this criterion the estimate of the height is

$$\tilde{h} = \overline{h} \pm \delta h$$

with a probability of 0.9.

The uncertainty in the height measurement defined by this criterion is a complex function of Δf noting that $\delta\phi$ is a function of α which is related to Δf through the correlation function. Referring to (23), it seems that the height uncertainty decreases when Δf is increased; however, it should also be noted that $\delta\phi$ increases when Δf is increased. This behavior suggests that there may exist a frequency shift Δf

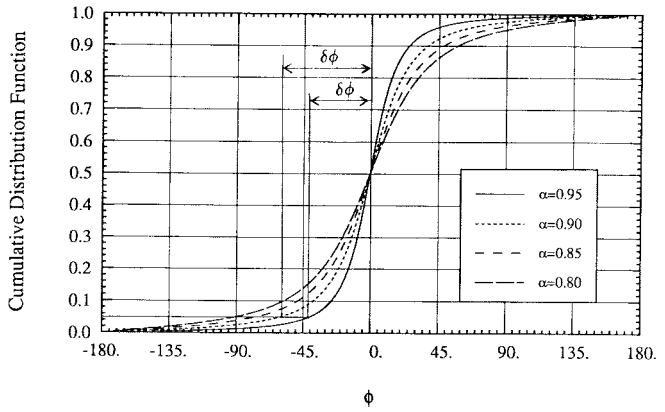

Fig. 4. Cumulative distribution function of the phase error for different values of α.

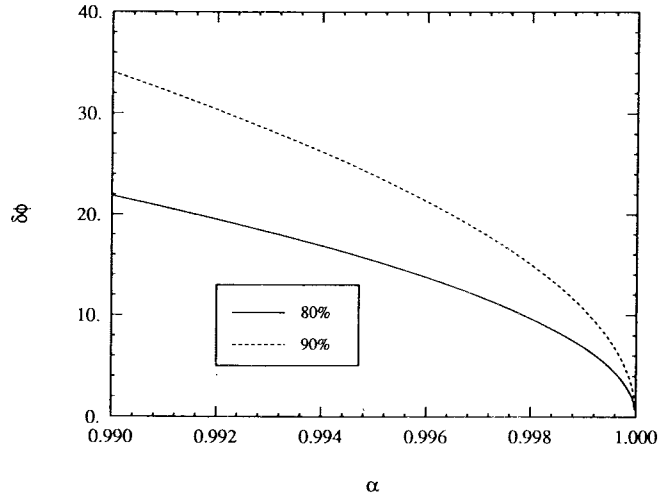

Fig. 5. The phase uncertainty for 80% and 90% percent error probability criteria as a function of α.

for which δh is minimized. This particular frequency shift will be referred to as the critical frequency shift. In order to investigate the possibility of finding the critical frequency shift, the relationship between the height uncertainty and the frequency shift must be obtained. The relationship between $\delta\phi$ and α can be directly obtained from the cumulative distribution function (cdf) of $\Delta\phi = \phi - \zeta$. Unfortunately, a close form for the cdf of $\Delta\phi$ does not exist and the relationship between $\delta\phi$ and α must be obtained numerically. Fig. 4 shows the cdf of $\Delta\phi$ for different values of α and the corresponding $\delta\phi$ for the 90% probability criterion. Note that for most practical cases $\alpha > 0.95$ (baseline distance or equivalently the frequency shift is rather small). The relationship between $\delta\phi$ and α is shown in Fig. 5 for the 80% and 90% probability criteria.

Assuming a Gaussian form for the normalized frequency correlation function the uncertainty in height estimation can easily be related to the frequency shift. Suppose the normalized frequency decorrelation function is given by

$$R(\Delta f) = e^{-(\Delta f/F_d)^2}$$

where F_d is the decorrelation bandwidth defined as the frequency shift for which $R(\Delta f) = e^{-1}$. Using (21) the frequency shift can be related to the degree of correlation through

$$\frac{\Delta f}{F_d} = \sqrt{-\ln(\alpha)}.$$

For values of α close to unity the right-hand side of the above equation is approximately equal to $\sqrt{1-\alpha}$. Referring to Fig. 5, it can also be observed that

$$\delta\phi \approx C\sqrt{1-\alpha}$$

where C is a constant proportional to the probability criterion. Therefore $\delta\phi$ is linearly proportional to Δf where upon substituting in (23) it can be shown that the height uncertainty is independent of the frequency shift and the critical frequency shift is not well defined. This result may be generalized to all frequency correlation functions because for small values frequency shift, the frequency correlation function of all targets can be approximated by

$$R(\Delta f) \approx 1 - (\Delta f/F_d)^2 \tag{24}$$

where F_d is a free parameter equal to the frequency decorrelation bandwidth of an equivalent Gaussian correlation function. Fig. 6 shows the product of the height uncertainty and the equivalent decorrelation bandwidth versus frequency shift normalized to the decorrelation bandwidth for both the 80% and 90% criteria. Thus the uncertainty in height measurement for a distributed target with known equivalent decorrelation bandwidth is independent of frequency shift or equivalently the baseline distance. In other words, the frequency decorrelation bandwidth of the target is the determining factor in the height measurement error.

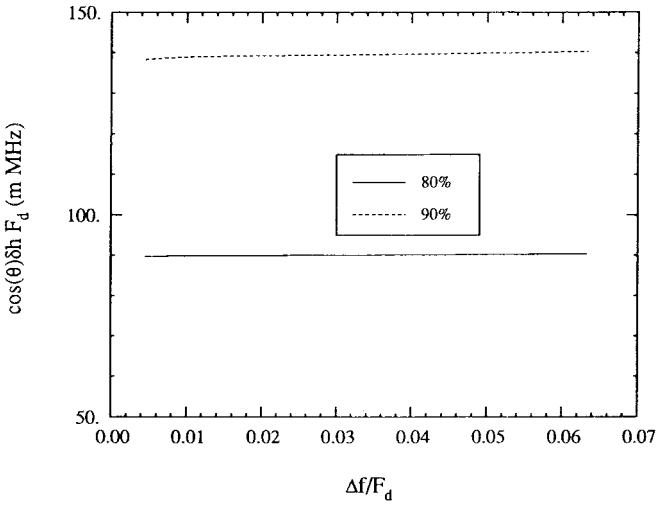

Fig. 6. Product of the height uncertainty and decorrelation bandwidth versus frequency shift normalized to the decorrelation bandwidth for a Gaussian correlation function.

IV. Frequency Correlation Function of Distributed Targets

As was shown in the previous section the frequency correlation function of a distributed target is the most important parameter in estimating its scattering phase center height. The literature concerning the frequency correlation function

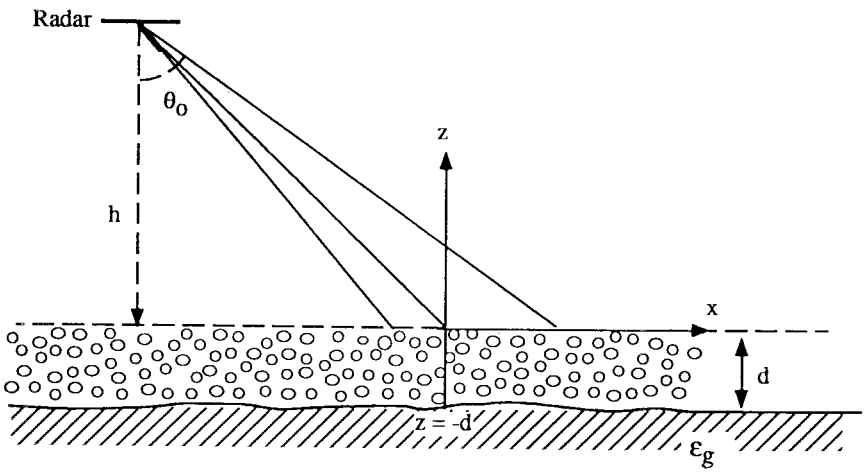

Fig. 7. Geometry of a homogeneous layer of random particles above a ground plane.

of distributed targets is rather scarce. Analytical expressions for the frequency correlation function of simple targets such as uniform independent scatterers and rough surfaces using Kirchhoff approximation have been obtained for simple uniform plane wave illuminations [18], [19]. For the uniform distribution of scatterers illuminated by a uniform plane wave the frequency correlation function is given by

$$R(\Delta f) = \frac{\sin(\pi \rho_r \Delta f/150)}{\pi \rho_r \Delta f/150}$$

where ρ_r is the slant range in meters and Δf is in megahertz. The corresponding Gaussian equivalent decorrelation bandwidth for this function is $F_d = 117/\rho_r$ MHz. Since product of δh and F_d is independent of $\Delta f/F_d$, the uncertainty in height measurement can be improved by decreasing the slant range resolution.

In a recent study [17] it was shown that the frequency correlation function, in general, depends on two sets of parameters: 1) radar parameters such as incidence angle, frequency, polarization, and footprint size, and 2) target parameters such as penetration depth and albedo. It is also shown that when the scattering is localized, that is, the field correlation distance in the random media is relatively small, the frequency correlation function can be expressed in terms of product of two expressions, one depending only on the radar parameters and the second one depending only on the target attributes. For example an expression for the frequency cross correlation of backscatter from a homogeneous layer of random particles such as leaves and stems above a smooth ground plane is found to be [17] where θ is the incident angle, d is the layer thickness, and R_p is the Fresnel reflection coefficient for p-polarized incident wave ($p \in v, h$). The first term in (25), shown at the bottom of the page, is the system dependent component in which G is the antenna gain or the SAR point-target response (ambiguity function), r is the radar distance, and the limits of the integrals represents the antenna footprint or the pixel area. The curly bracket in equation (25) represents the target dependent component in which κ denotes the layer extinction and W^b_{pppp} and W^s_{pppp} are the copolarized components of the phase matrix in the backscatter and specular (with respect to the vertical axis) directions which are defined by

$$W^{b,s}_{pppp} = \lim_{\Delta V \to 0} \frac{\langle (\Delta S^{b,s}_{pp})(\Delta S^{b,s}_{pp})^* \rangle}{\Delta V}, p \in v, h$$

where ΔS_{pp} represents a scattering matrix element of a small volume ΔV of the random medium. In the expression given by (25) the reference phase plane is assumed to be at the top of the layer, i.e., the ground plane is assumed to be at $z = -d$ as shown in Fig. 7.

The decorrelation caused by the system-dependent component for an imaging radar is directly proportional to the system slant range resolution. Also for conventional radars the decorrelation caused by the system component is inversely proportional to antenna beamwidth and directly proportional to range and incidence angle. In most existing INSAR systems the measured decorrelation is dominated by the system component. As discussed before the uncertainty in height estimation increases as the correlation bandwidth increases. Fortunately the decorrelation caused by the system parameters can be calibrated out since its effect appears as a simple multiplicative factor. If the system ambiguity function or the antenna pattern is known, the system component of frequency correlation function can easily be computed and removed from the measured data. In cases where the ambiguity function or the antenna pattern is not well characterized the correlation over a rough surface (a distributed target with no vertical extent) approximately represents the system component of the decorrelation and can be used for calibration. Once the target

$$\langle E_{pp}(f_2) E^*_{pp}(f_2) \rangle = \left[\iint \frac{e^{2i\Delta k r(x,y)}}{r^4(x,y)} |G(x,y)|^2 \, dx \, dy \right] \cdot \left\{ 4d|R_p|^2 W^s_{pppp} e^{2(i\Delta k \cos\theta - \kappa \sec\theta)d} + W^b_{pppp}(1 + |R_p|^4 e^{2(i\Delta k \cos\theta - \kappa \sec\theta)d}) \frac{1 - e^{2(i\Delta k \cos\theta - \kappa \sec\theta)d}}{2(\kappa \sec\theta - i\Delta k \cos\theta)} \right\} \quad (25)$$

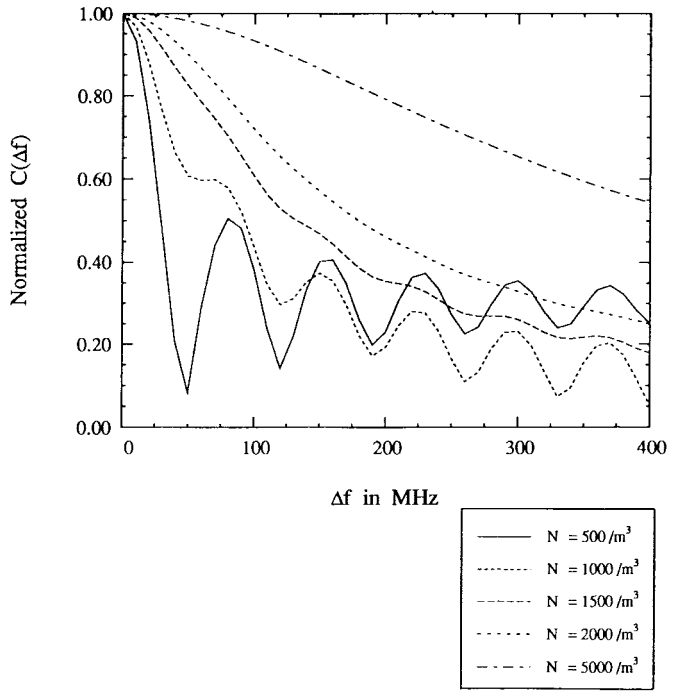

Fig. 8. Frequency correlation function of a 2-m thick random layer of flat leaves with average area 50 cm^2, thickness 1.3 mm, and dielectric constant $\epsilon_l = 19 + i6.3$ above a ground plane with $\epsilon_g = 15 + j2$ at 5.3 GHz and $\theta = 30°$ (note for INSAR case $\Delta f < 1$ MHz).

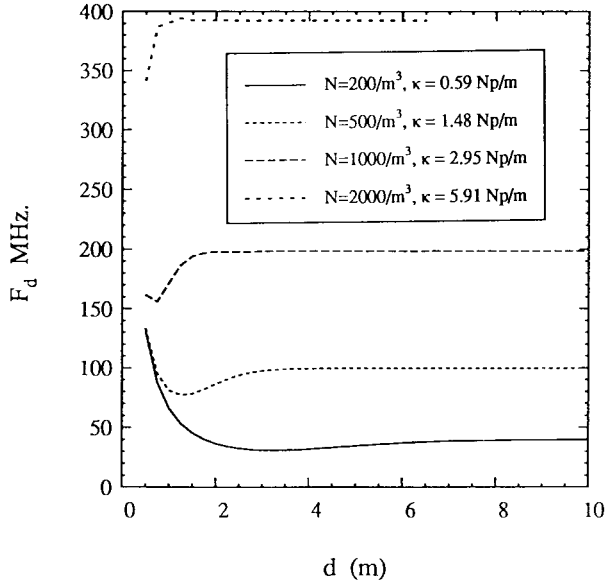

Fig. 9. Gaussian equivalent decorrelation bandwidth of the layer as a function of depth for different values of particle number density at $f = 5.3$ GHz and $\theta = 30°$.

dependent component of the correlation function is obtained, the equivalent frequency decorrelation bandwidth can be computed from which the uncertainty in height estimation can be evaluated. As shown in the simple model described by (25) the target decorrelation contains information about its physical parameters.

Fig. 8 shows the frequency correlation function of a uniform random layer of flat leaves with average area 50 cm^2, thickness 1.3 mm, and dielectric constant $\epsilon_l = 19 + i6.3$ above a ground plane with dielectric constant $\epsilon_g = 15 + j2.0$ at 5.3 GHz and incidence angle $\theta = 30°$. In this simulation the layer thickness was chosen to be $d = 2m$ and leaf number density N_0 was varied as a parameter. It is shown that as the leaf number density, and as a direct result the extinction, increases the frequency decorrelation bandwidth increases. Scattering contributions from the ground bounce mechanisms are manifested in terms of oscillations on the frequency correlation function due to constructive and destructive interferences among the different scattering mechanisms. Existence of contribution from ground bounce scattering mechanisms significantly reduce the frequency decorrelation bandwidth. For interferometric SAR's the equivalent frequency shift is rather small (<1 MHz) and the approximate form of the frequency correlation function given by (24) seems to be adequate for all cases. Fig. 9 shows F_d of the layer as a function of depth for different values of particle number density. As the vegetation depth decreases F_d should approach infinity and when the vegetation depth increases F_d reaches its asymptotic value for the corresponding to a semi-infinite medium.

The theoretical expression for the frequency cross correlation function given by (25) can be used to calculate the height of the scattering phase center above the ground plane. Substituting the phase of the target dependent term of (25) in (22), the mean height of the scattering phase center of the medium can be computed. Fig. 10(a) and (b) show the height of the scattering phase center of the uniform medium as a function of layer thickness and extinction for 30° and 60° incidence angles respectively. It is shown that depending on the layer thickness, extinction, and incidence angle the scattering phase center may appear below or above the ground plane, but always below the canopy top. Note that when the double-bounce scattering mechanism (ground-target-ground) is dominant, the scattering phase center appears below the ground plane. Other numerical simulations showed that particle orientation distribution can significantly influence the location of the scattering phase center as well. This is due to the fact that the relative contribution of the direct backscatter mechanism with respect to that of the double-bounce scattering mechanism is a function of particle orientation distribution.

To illustrate the ability of INSAR in retrieving vegetation parameters, let us consider a simple case of semi-infinite uniform medium. Vegetation canopy can be regarded as a semi-infinite medium, when canopy transmissivity is below 0.1. In this case an analytical expression for frequency correlation function and the phase of the frequency cross correlation (mean phase) can be obtained directly from (25) by settin $\kappa\sec(\theta) = \infty$. The expression for the frequency correlation function and the mean phase are, respectively, given by

$$R(\Delta f) = \frac{1}{\sqrt{1 + \left(\frac{2\pi\Delta f}{c\kappa}\right)^2}} \approx 1 - \left(\frac{\pi\Delta f}{2c\kappa}\right)^2 \quad (26)$$

$$\zeta = \tan^{-1}\frac{\Delta k\cos^2\theta}{\kappa} \approx \frac{\Delta k\cos^2\theta}{\kappa}. \quad (27)$$

Using (26) the extinction coefficient of a thick vegetation layer can be obtained as follows. For a system with a known baseline

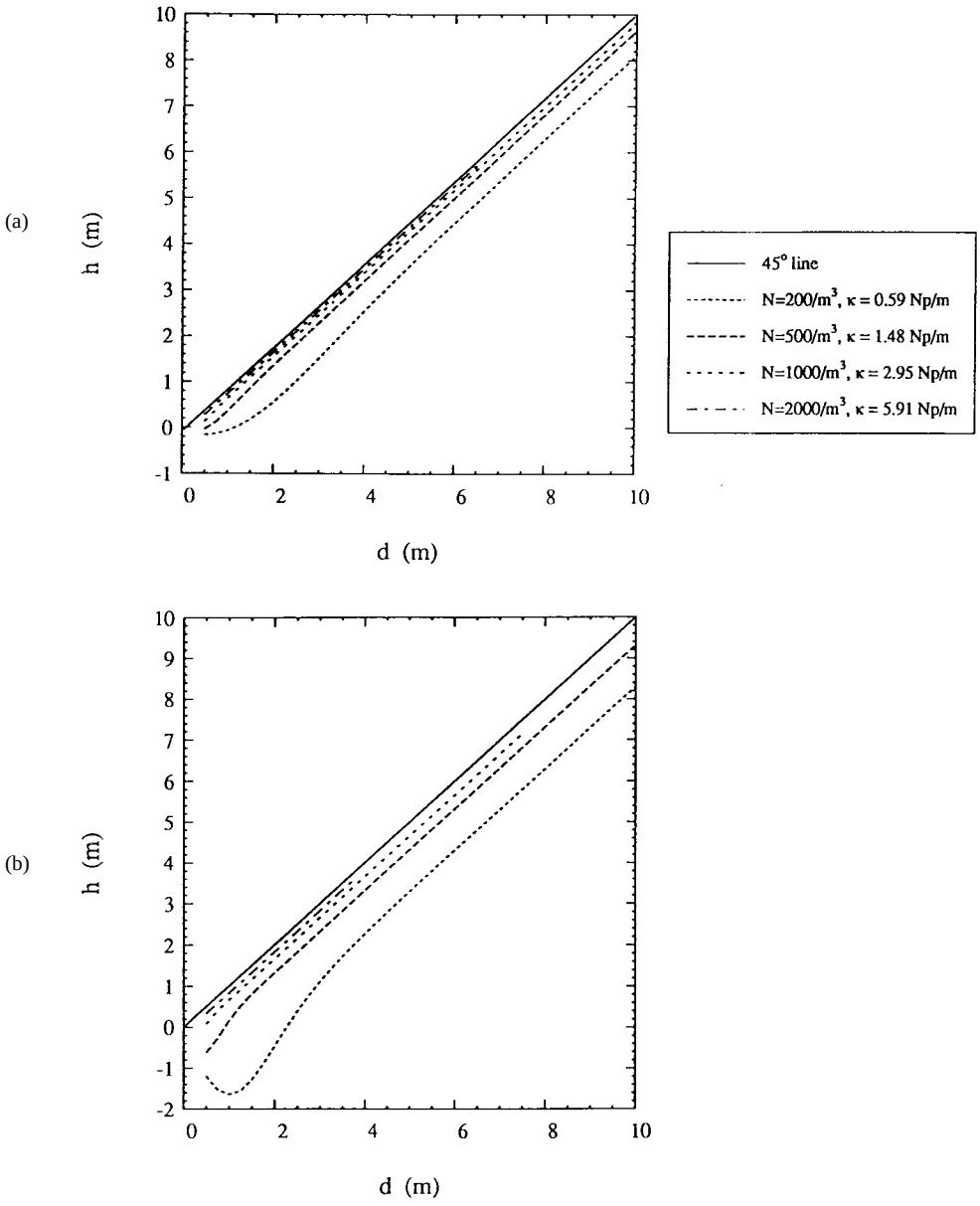

Fig. 10. Height of the scattering phase center of the layer above the ground as a function of layer thickness for different values of particle density at $f = 5.3$ GHz. (a) $\theta = 30^\circ$ and (b) $\theta = 60^\circ$.

distance the equivalent Δf can be calculated from (5) which together with the measured decorrelation can be substituted in (26) to calculate κ. Having found κ, (27) can be substituted in (22) to calculate the location of the scattering phase center from the canopy top Δd which is given by

$$\Delta d = \frac{\cos\theta}{2\kappa}. \tag{28}$$

It should be noted that for forest stands where particle size orientation and distribution are highly nonuniform the simple uniform and homogeneous model described above may not provide satisfactory results. More accurate models that preserve the effect of tree structure are needed for this purpose. A coherent scattering model based on Monte Carlo simulation of fractal generated trees is under development which allows efficient and accurate computation of frequency cross correlation statistics.

V. Conclusions

In this paper theoretical and statistical relationships between the measured parameters obtained from an interferometric SAR, namely the phase and correlation coefficient of interferogram, and target parameters are obtained. First an equivalent relationship between an INSAR and a Δk radar is established. It is shown that the knowledge of the frequency correlation behavior of radar backscatter is sufficient to derive the desired statistics of height estimation using an interferometric SAR. The equivalence relationship allows for conducting controlled experiments, using a scatterometer, to characterize the response of a distributed target when imaged by an INSAR. Similarly efficient numerical codes can be developed to simulate the results. Statistical analysis shows that the uncertainty in the height estimation of a distributed target is a function of equivalent frequency decorrelation

bandwidth and is independent of the baseline distance. It was also shown that how the INSAR measured parameters can be used to evaluate the extinction, the physical height, and the height of the scattering phase center of a closed and uniform semi-infinite canopy.

REFERENCES

[1] K. Sarabandi, "Electromagnetic scattering from vegetation canopies," Ph.D. dissertation, Univ. Michigan, Ann Arbor, 1989.

[2] F. T. Ulaby, K. Sarabandi, K. McDonald, M. Whitt, and M. C. Dobson, "Michigan microwave canopy scattering model," *Int. J. Remote Sensing*, vol. 11, no. 7, 1223–1253, July 1990.

[3] M. C. Dobson, F. T. Ulaby, L. E. Pirece, T. L. Sharik, K. M. Bergen, J. Kellndorfer, J. R. Kendra, E. Li, Y. C. Lin, A. Nashashibi, K. Sarabandi, and P. Siqueira, "Estimation of forest biomass," *IEEE Trans. Geosci. Remote Sensing.*, vol. 33, pp. 887–895, July 1995.

[4] K. J. Ranson, S. Saatchi, and G. Sun, "Boreal forest ecosystem characterization with SIR-C/X SAR," *IEEE Trans. Geosci. Remote Sensing.*, vol. 33, no. 4, pp. 867–876, July 1995.

[5] H. A. Zebker, S. N. Madsen, J. Martin, K. B. Wheeler, T. Miller, Y. Lou, G. Alberti, S. Vetrella, and A. Cucci, "The TOPSAR interferometric radar topographic mapping instrument," *IEEE Trans. Geosci. Remote Sensing*, vol. 30, pp. 933–940, Sept. 1992.

[6] F. K. Li, and R. M. Goldstein, "Study of multibaseline spaceborne interferometric synthetic aperture radars," *IEEE Trans. Geosci. Remote Sensing*, vol. 28, pp. 88–97, Jan. 1990.

[7] A. L. Gray and P. J. Farris-Manning, "Repeat-pass interferometry with airborne synthetic aperture radar," *IEEE Trans. Geosci. Remote Sensing*, vol. 31, pp. 180–191, Jan. 1993.

[8] A. K. Gabriel and R. M. Goldstein, "Crossed orbit interferometry: Theory and experimental results from SIR-B," *Int. J. Remote Sensing*, vol. 9, no. 5, pp. 857–872, 1988.

[9] S. N. Madsen, H. A. Zebker, and J. Martin, "Topographic mapping using radar interferometry: Processing techniques," *IEEE Trans. Geosci. Remote Sensing*, vol. 31, pp. 246–256, Jan. 1993.

[10] E. Rodriguez and J. M. Martin, "Theory and design of interferometric synthetic aperture radars," *Proc. Inst. Elect. Eng.*, vol. F139, no. 2, pp. 147–159, 1992.

[11] H. A. Zebker and J. Villasenor, "Decorrelation in Interferometric Radar Echoes," *IEEE Trans. Geosci. Remote Sensing*, vol. 30, pp. 950–959, Sept. 1992.

[12] J. O. Hagberg, L. M. H. Ulander, and J. Askne, "Repeat-pass SAR interferometry over forested terrain," *IEEE Trans. Geosci. Remote Sensing*, vol. 33, pp. 331–340, Mar. 1995.

[13] W. B. Davenport, *Probability and random processes*, New York: McGraw-Hill, 1970.

[14] K. Sarabandi, "Derivation of phase statistics of distributed targets from the Mueller matrix," *Radio Sci.*, vol. 27, no. 5, pp 553–560, 1992.

[15] I. R. Joughin, D. P. Winebrenner, and D. B. Percival, "Probability density functions for multilook polarization signatures,"*IEEE Trans. Geosci. Remote Sensing*, vol. 32, pp. 562–574, May 1994.

[16] J. Lee, K. W. Hoppel, S. A. Mango, A. R. Miller, "Intensity and phase statistics of multilook polarimetric and interferometric SAR imagery," *IEEE Trans. Geosci. Remote Sensing*, vol. 32, pp. 1017–1028, Sept. 1994.

[17] K. Sarabandi and A. Nashashibi, "Analysis and applications of backscattered frequency correlation function," *IEEE Trans. Antennas Propagat.*, submitted for publication.

[18] W. P. Brikemeier and N. D. Wallace, "Radar tracking accuracy improvement by means of pulse to pulse frequency modulation," *IEEE Trans. Commun. Electron.*, no. 1, pp. 571–575, Jan. 1963.

[19] A. A. Monakov, J. Vivekanandan, A. S. Stjernman, and A. K. Nystrom, " Spatial and frequency averaging techniques for a polarimetric scatterometer system," *Trans. Geosci. Remote Sensing*, vol. 32, pp. 187–196, Jan. 1994.

Kamal Sarabandi (S'87–M'90–SM'93), for a photograph and biography, see this issue, p. 1231.